Acta Crystallographica Section A
Foundations of Crystallography
ISSN 0108-7673

Received 20 December 2000
Accepted 14 February 2001

A proposal for a transition mechanism from the diamond to the lonsdaleite type

H. Sowa[a] and E. Koch[b]*

[a]Institut für Angewandte Geowissenschaften, Allgemeine und Angewandte Mineralogie, Technische Universität BH1, Ernst-Reuter-Platz 1, D-10587 Berlin, Germany, and [b]Institut für Mineralogie, Petrologie und Kristallographie der Philipps-Universität Marburg, Hans-Meerwein-Strasse, D-35032 Marburg, Germany. Correspondence e-mail: kochelke@mailer.uni-marburg.de

A phase transition between the diamond ($Fd\bar{3}m$) and the lonsdaleite types ($P6_3/mmc$) may be described as a deformation of a homogeneous sphere packing with three contacts per sphere (type 3/10/o1) in the common subgroup $Pnna$ of $Fd\bar{3}m$ and $P6_3/mmc$. The frequently observed transition between the zinc-blende ($F\bar{4}3m$) and the wurtzite types ($P6_3mc$) may be described in an analogous way as a deformation of a heterogeneous sphere packing in the subgroup $Pna2_1$. The proposed model guarantees the three-dimensional connection during the whole transformation process. By this property it is distinguished from other models.

1. Introduction

A transition between diamond-type and lonsdaleite-type (hexagonal diamond) structures can be induced in silicon wafers either by deformations as a result of indentation (Eremenko & Nikitenko, 1972) or by implantation of ions (Tan *et al.*, 1981). Tan *et al.* (1981) presented a detailed description of a possible transition mechanism that explains the observed orientation relations between the two phases.

Their structure types are closely related to the zinc-blende and to the wurtzite type, respectively. Whereas diamond- and lonsdaleite-type structures contain only one kind of atom, structures with the zinc-blende and wurtzite types are built up of two different kinds. With the exception of some mercury chalcogenides, AB compounds with four-coordinated atoms crystallize either with zinc-blende- or with wurtzite-type structures, depending on the ionicity. If the atoms show large differences in electronegativity, the wurtzite type is preferred, while compounds with mainly covalent bonds form zinc-blende-type structures. Intermediate compounds may occur with both structure types at ambient conditions. In order to determine the stable phases, Yeh *et al.* (1992) calculated the energy differences between the zinc-blende and the wurtzite type for 13 binary semiconductors. Phase transformations between the zinc-blende and the wurtzite type have often been observed. For instance, ZnS undergoes a corresponding transition at about 1293 K (Allen & Crenshaw, 1913). Although in both structure types the neighbourhood of all atoms is very similar, the structures are topologically different, and it is not possible to deform them into each other without breaking bonds and forming new ones. Therefore, the phase transition is reconstructive. Nevertheless, single crystals can be preserved during the transformation (Allen & Crenshaw, 1913; Shôji, 1933). Some papers deal with the corresponding transition mechanism: Shôji (1931) proposed a model in which planes of atoms perpendicular to one of the ⟨111⟩ directions of zinc blende are shifted with respect to one another. He verified that this mechanism takes place by taking Laue diffraction photographs before and after the phase transition (Shôji, 1933). Sebastian *et al.* (1982) investigated the transformation from wurtzite to zinc blende on single crystals. They took oscillation photographs at room temperature after annealing the ZnS crystals for 1 h at successively higher temperatures. The authors found that the transition starts with the insertion of deformation faults. By analysing experimental data on the wurtzite to zinc-blende transformation, Pandey & Lele (1986) inferred that shearing processes occur and, therefore, this transition is martensitic.

The transition between the SiO_2 modifications high-cristobalite and high-tridymite may also be related to the transition from the diamond to the lonsdaleite type, as the Si atoms in these structures form a diamond and a londsdaleite configuration, respectively. The O atoms are located in the middle between all neighbouring Si atoms, so that each Si atom has four O neighbours and each O atom has two Si neighbours. The crystal structures of ice I_c and ice I_h belong to the high-cristobalite type and the high-tridymite type, respectively, and a corresponding phase transition that depends on temperature has also been observed (*cf.* Shallcross & Carpenter, 1957).

Quite recently, possible transition models for pressure-induced phase transformations in AB compounds have been derived in investigating the symmetry relations between low- and high-pressure phases. These studies include the transitions from the NaCl to the CsCl type (Sowa, 2000*a*), from the zinc-blende to the NaCl type (Sowa, 2000*b*), and from the wurtzite to the NaCl type (Sowa, 2001). All these transformations are

described as being displacive because no bonds have to be broken and only relatively small atomic shifts in combination with metrical changes are necessary.

In the present study, an attempt is made to provide a similar description of a reconstructive phase transition that implies breaking of part of the bonds.

2. Symmetry relations

For the following investigations, the assumption is made that only one kind of atom exists and that the corresponding structures form homogeneous sphere packings, *i.e.* the transformation between diamond and lonsdaleite types is considered. The results can easily be transferred to binary compounds.

The diamond structure is described with symmetry $Fd\bar{3}m$. It corresponds to the cubic invariant lattice complex *cD* (*International Tables for Crystallography*, 1995, Vol. A, ch. 14) and to a homogeneous sphere packing of type 4/6/*c*1 (Fischer, 1973; for symbols of sphere packings, see §3) with four contacts per sphere. The atoms occupy the positions 8(*a*) $\bar{4}3m$ 0,0,0 (referred to origin choice 1).

Lonsdaleite crystallizes in space group $P6_3/mmc$. The atomic arrangement corresponds to a configuration of the hexagonal univariant lattice complex *E*2*z* (*International Tables for Crystallography*, 1995, Vol. A, ch. 14) and to a homogeneous sphere packing of type 4/6/*h*2 (Fischer & Koch, unpublished; *cf.* Fischer & Koch, 1994) that also has contact number four. The atoms are situated at Wyckoff position 4(*f*) 3*m*. $\frac{1}{3},\frac{2}{3},z$ with $z=\frac{1}{16}$. The ideal atomic arrangement is obtained for an axial ratio $c/a=\frac{2}{3}\times 6^{1/2}\cong 1.633$.

The corresponding binary compounds *AB* crystallize in the zinc-blende type with space group $F\bar{4}3m$ where the atoms occupy the positions 4(*a*) $\bar{4}3m$ 0,0,0 and 4(*c*) $\bar{4}3m$ $\frac{1}{4},\frac{1}{4},\frac{1}{4}$, or in the wurtzite type with space group $P6_3mc$ where the atoms are located at Wyckoff position 2(*b*) 3*m*. $\frac{1}{3},\frac{2}{3},z$ with $z=0$ and $z=\frac{3}{8}$, respectively. In both structure types, the *A* and *B* atoms together form heterogeneous sphere packings with four contacts per sphere.

One may ask for a model of the phase transition from the diamond to the lonsdaleite type that leaves all atoms symmetrically equivalent and that preserves the three-dimensional connection of the crystal structure during the transition. Then, only one bond per atom is allowed to break and the linkage of the atoms in the intermediate phase can be described by a sphere packing with three contacts. There exists only one lattice complex that enables such a transition. It corresponds to the general position 8(*e*) *x*,*y*,*z* of *Pnna* and contains *cD* as well as *E*2*z* as limiting complexes (*cf.* Fig. 1). Furthermore, three nearest neighbours in the diamond configuration are equivalent to three nearest neighbours in the ideal lonsdaleite arrangement and, in fact, a corresponding three-connected sphere packing has been described in *Pnna* (Koch & Fischer, 1995). It belongs to type 3/10/*o*1. The undistorted diamond type is found in *Pnna* 8(*e*) *x*, *y*, *z* with $x=\frac{1}{8}$, $y=\frac{1}{8}$, $z=0$ and $a/c=2$ and $b/c=2^{1/2}$, while, with $x=\frac{1}{12}$, $y=\frac{1}{16}$, $z=\frac{1}{4}$ and $a/c=3^{1/2}$ and $b/c=\frac{2}{3}\times 6^{1/2}$, the ideal lonsdaleite type is realized.

The analogous transition in *AB* compounds can be described in the subgroup $Pna2_1$ of *Pnna* (Fig. 2) where the zinc-blende and the wurtzite types occur with the following positional parameters and axial ratios: *A* in 4(*a*) $x=\frac{1}{8}$, $y=\frac{1}{4}$, $z=0$, *B* in 4(*a*) $x=\frac{3}{8}$, $y=\frac{1}{4}$, $z=\frac{3}{4}$ and $a/c=2^{1/2}$ and $b/c=\frac{1}{2}\times 2^{1/2}$ lead to the undistorted zinc-blende type, whereas *A* in 4(*a*) $x=\frac{1}{3}$, $y=0$, $z=0$ and *B* in 4(*a*) $x=\frac{1}{3}$, $y=0$, $z=\frac{5}{8}$ and $a/c=\frac{3}{4}\times 3^{1/2}$ and $b/c=\frac{1}{4}\times 6^{1/2}$ give the ideal wurtzite type. The three-connected sphere packing, the deformation of which leads either to the zinc-blende or to the wurtzite type, is a heterogeneous one.

3. Sphere packings in the surroundings of 3/10/*o*1

In the following, each sphere-packing type is designated by a symbol *k*/*m*/*fn* as was first introduced by Fischer (1971): *k* means the number of contacts per sphere, *m* is the length of the shortest mesh within the sphere packing, *f* indicates the highest crystal family for a sphere packing of that type (*c*: cubic; *t*: tetragonal; *h*: hexagonal/trigonal; *o*: orthorhombic), and *n* is an arbitrary number.

Sphere packings of type 3/10/*o*1 can solely be generated within the general position of *Pnna* (*cf.* Koch & Fischer, 1995), *i.e.* within a five-dimensional parameter field (three coordi-

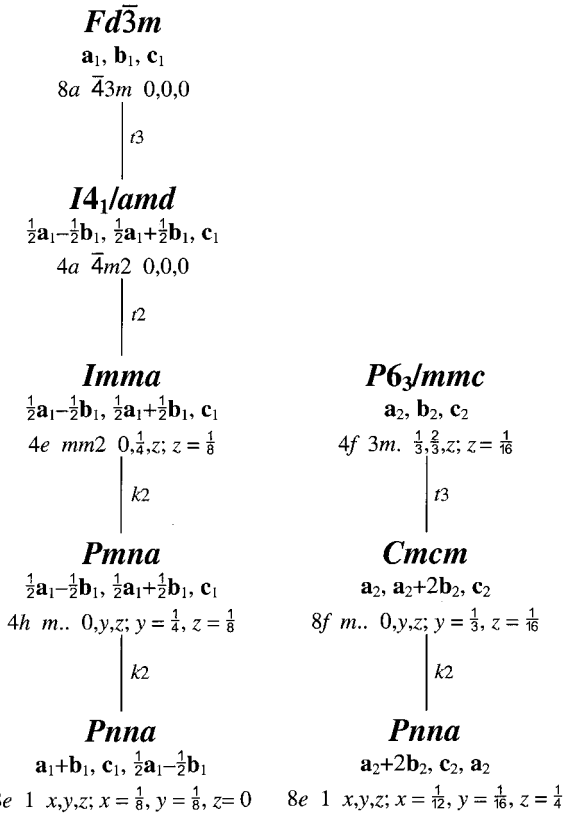

Figure 1
Symmetry relation between the crystal structures of diamond and of lonsdaleite. The transition from $I4_1/amd$ to *Imma* requires an origin shift by $(0,-\frac{1}{4},-\frac{1}{8})$ with reference to the basis of $I4_1/amd$; the transition from *Cmcm* to *Pnna* requires a shift by $(-\frac{1}{4},-\frac{1}{4},0)$ with reference to the basis of *Cmcm*.

nates and two axial ratios). Such a sphere packing occurs if the original sphere with centre at x,y,z has three symmetrically equivalent and equidistant neighbours with centres at $-x, -y, -z$, at $x, \frac{1}{2}-y, \frac{1}{2}-z$, and at $\frac{1}{2}-x, -y, z$ and squared distances $d_A^2 = 4x^2a^2 + 4y^2b^2 + 4z^2c^2$, $d_B^2 = (\frac{1}{2}-2y)^2b^2 + (\frac{1}{2}-2z)^2c^2$ and $d_C^2 = (\frac{1}{2}-2x)^2a^2 + 4y^2b^2$, respectively. Equating the squared distances yields the sphere-packing conditions for the type 3/10/*o*1,

$$\begin{aligned} 16x^2a^2 + (8y-1)b^2 + (8z-1)c^2 &= 0, \\ 16z^2c^2 + (8x-1)a^2 &= 0. \end{aligned} \qquad (1)$$

Therefore, the parameter region of type 3/10/*o*1 has three degrees of freedom. It is bounded by 38 parameter regions with fewer degrees of freedom belonging to 30 other types of sphere packing with additional sphere contacts. In Fig. 3, the parameter region for type 3/10/*o*1 together with its boundaries is schematically represented by the Schlegel diagram of a polyhedron with eight faces, 18 edges and 12 vertices. The interior of this polyhedron corresponds to the parameter region of 3/10/*o*1 whereas the faces, edges and vertices belong to the adjacent parameter regions of sphere-packing types

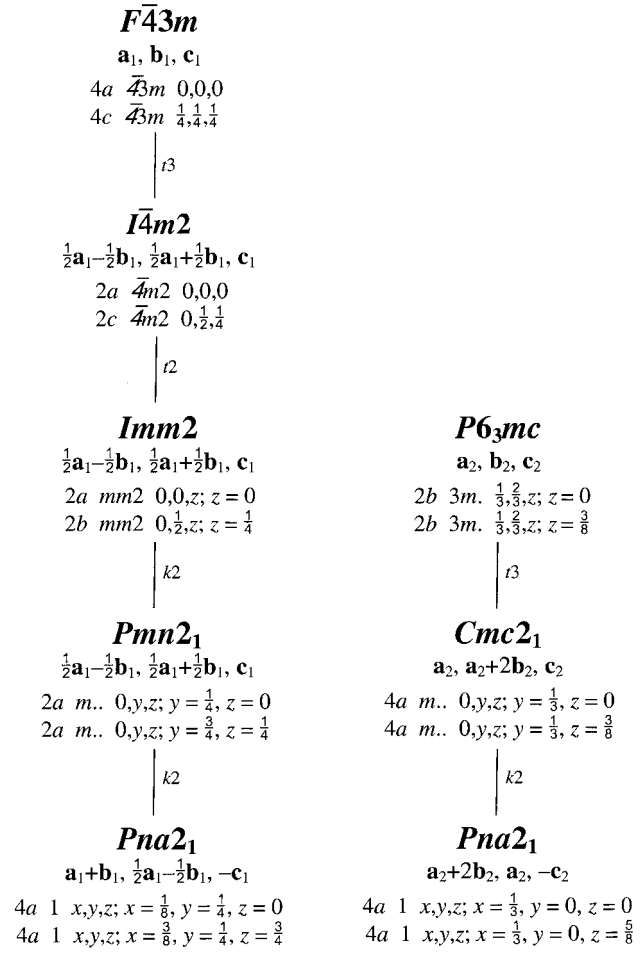

Figure 2
Symmetry relation between the crystal structures of zinc blende and of wurtzite. The transition from *Imm*2 to *Pmn*2$_1$ requires an origin shift by $(0, -\frac{1}{4}, 0)$ with reference to the basis of *Imm*2; the transition from *Pmn*2$_1$ to *Pna*2$_1$ requires a shift by $(-\frac{1}{4}, 0, 0)$ with reference to the basis of *Pmn*2$_1$.

Table 1
Symmetry operations and coordinates of neighbouring points that may give rise to sphere contacts if the original sphere is located in the interior or at the boundary of the parameter field of type 3/10/*o*1.

Neighbour	Coordinates	Symmetry operation
A	$-x, -y, -z$	$\bar{1}(0, 0, 0)$
B	$x, \frac{1}{2}-y, \frac{1}{2}-z$	$2(x, \frac{1}{4}, \frac{1}{4})$
C	$\frac{1}{2}-x, -y, z$	$2(\frac{1}{4}, 0, z)$
D	$x, \frac{1}{2}-y, -\frac{1}{2}-z$	$2(x, \frac{1}{4}, -\frac{1}{4})$
E	$x, y, 1+z$	$t(0, 0, 1)$
	$x, y, -1+z$	$t(0, 0, -1)$
F	$-x, -y, 1-z$	$\bar{1}(0, 0, \frac{1}{2})$
G	$x, -\frac{1}{2}-y, \frac{1}{2}-z$	$2(x, -\frac{1}{4}, \frac{1}{4})$
H	$x, 1+y, z$	$t(0, 1, 0)$
	$x, -1+y, z$	$t(0, -1, 0)$
I	$-x, 1-y, -z$	$\bar{1}(0, \frac{1}{2}, 0)$
J	$\frac{1}{2}-x, 1-y, z$	$2(\frac{1}{4}, \frac{1}{2}, z)$
K	$\frac{1}{2}+x, y, -z$	$a(x, y, 0)$
	$-\frac{1}{2}+x, y, -z$	
L	$-\frac{1}{2}-x, -y, z$	$2(-\frac{1}{4}, 0, z)$
M	$\frac{1}{2}+x, y, 1-z$	$a(x, y, \frac{1}{2})$
	$-\frac{1}{2}+x, y, 1-z$	
N	$x, -\frac{1}{2}-y, -\frac{1}{2}-z$	$2(x, -\frac{1}{4}, -\frac{1}{4})$
O	$-\frac{1}{2}-x, 1-y, z$	$2(-\frac{1}{4}, \frac{1}{2}, z)$

with two degrees of freedom (2.1 to 2.8) or with one (1.1 to 1.18) or with no (0.1 to 0.12) degree of freedom, respectively.

Table 1 displays all symmetry operations that may give rise to a contact between the original and a neighbouring sphere if the former is located somewhere in the interior or at the boundary of the parameter field of type 3/10/*o*1. All sphere-packing types in the surroundings of 3/10/*o*1 are listed in Table 2. The symbol *p.q* in the first column gives the number *p* of degrees of freedom of the corresponding parameter region and an arbitrary numbering *q*. The second column refers to Table 1 and identifies the centres of the neighbouring spheres and the corresponding symmetry operations. The third column shows the simplest (but not all) parameter conditions that have to be fulfilled in addition to (1). In column 4, the respective sphere-packing type is designated by its symbol *k*/*m*/*fn*. As sphere packings of most of the types may also be

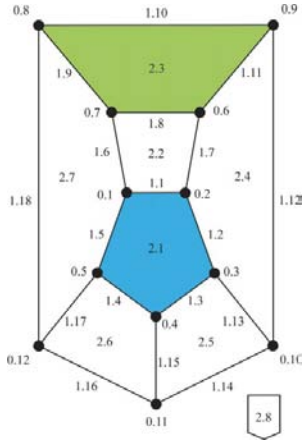

Figure 3
Sphere packings in the surroundings of 3/10/*o*1.

generated within some supergroup of *Pnna*, the last column shows the highest possible symmetry for each type.

Most of the sphere-packing types listed in Table 2 have been described before: 3/10/*o*1 by Koch & Fischer (1995); 4/6/*c*1 by Fischer (1973); 5/4/*t*6, 6/4/*t*2, 8/3/*t*1 and 9/3/*t*2 by Fischer (1991*a*); 6/3/*t*5 by Fischer (1991*b*); 6/3/*o*1 and 8/3/*h*4 by Sowa (2000*b*); 4/6/*h*2, 5/4/*h*5, 10/3/*h*2, 6/3/*o*2, 7/3/*o*1, 7/4/*o*1, 8/3/*o*2 and 9/3/*o*1 by Sowa (2001). The 13 further types occur only within the orthorhombic crystal system and have not been mentioned before.

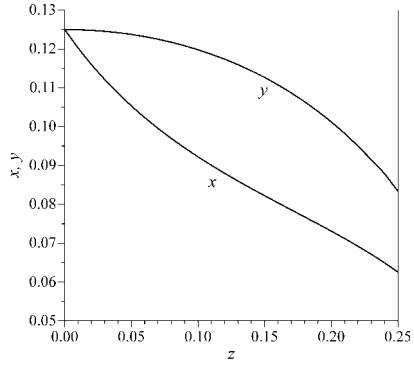

Figure 4
Variations of the coordinate parameters x and y depending on z along the proposed transition path.

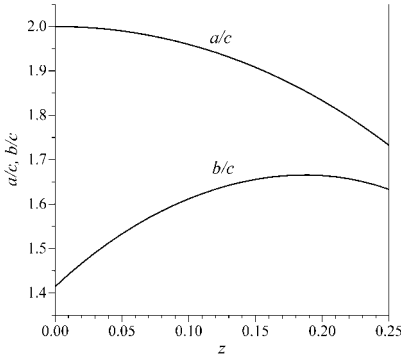

Figure 5
Variations of the axial ratios a/c and b/c depending on z along the proposed transition path.

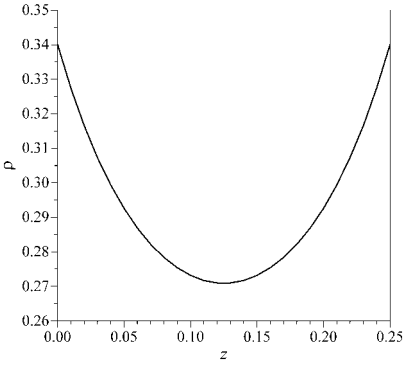

Figure 6
Variation of the sphere-packing density ρ depending on z along the proposed transition path.

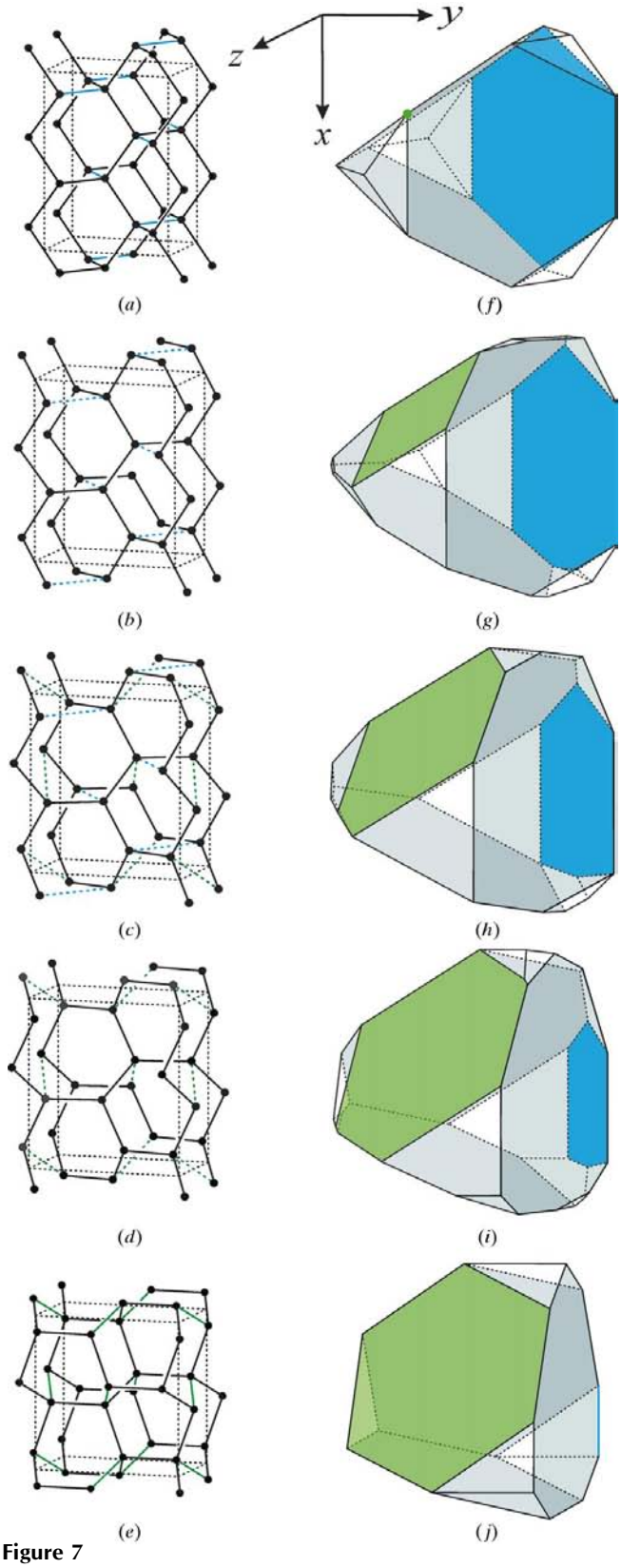

Figure 7
Sphere-packing deformations (*a*)–(*e*) and deformations of the corresponding Dirichlet domains (*f*)–(*j*) along the proposed transition path for different values of z. (*a*), (*f*) $z = 0$; (*b*), (*g*) $z = \frac{1}{16}$; (*c*), (*h*) $z = \frac{1}{8}$; (*d*), (*i*) $z = \frac{3}{16}$; (*e*), (*j*) $z = \frac{1}{4}$. Blue and green lines in (*a*)–(*e*) show the breaking bonds in the diamond and the ideal lonsdaleite configurations, respectively. Accordingly, the blue and green coloured parts of the Dirichlet domains in (*f*)–(*j*) are caused by the lost neighbours.

Table 2
Sphere-packing types in the surroundings of 3/10/*o*1.

	Neighbouring points	Additional conditions	Sphere-packing type	Maximal symmetry
3.1	*ABC*		3/10/*o*1	*Pnna* 8(*e*)
2.1	*ABCD*	$x = \frac{1}{8}$, $z = 0$	4/6/*c*1	$Fd\bar{3}m$ 8(*a*)
2.2	*ABCE*	$c = 1$	5/4/*o*2	*Pnna* 8(*e*)
2.3	*ABCF*	$z = \frac{1}{4}$	4/6/*h*2	$P6_3/mmc$ 4(*f*)
2.4	*ABCG*	$y = 0$	4/4/*o*1	*Imma* 8(*h*)
2.5	*ABCH*	$b = 1$	5/4/*o*3	*Pnna* 8(*e*)
2.6	*ABCIJ*	$y = \frac{1}{4}$	5/4/*o*1	*Cmcm* 8(*g*)
2.7	*ABCK*		5/3/*o*1	*Pnna* 8(*e*)
2.8	*ABCL*	$x = 0$	4/4/*o*2	*Cccm* 8(*l*)
1.1	*ABCDE*	$x = \frac{1}{8}$, $z = 0$; $c = 1$	6/3/*o*1	*Imma* 4(*e*)
1.2	*ABCDGN*	$x = \frac{1}{8}$, $y = z = 0$; $a = 4$	6/4/*c*1	$Pm\bar{3}m$ 1(*a*)
1.3	*ABCDH*	$x = \frac{1}{8}$, $z = 0$; $b = 1$	6/4/*t*2	$I4_1/amd$ 4(*a*)
1.4	*ABCDIJ*	$x = \frac{1}{8}$, $y = \frac{1}{4}$, $z = 0$; $c = 2$	6/4/*c*1	$Pm\bar{3}m$ 1(*a*)
1.5	*ABCDK*	$x = \frac{1}{8}$, $z = 0$; $a = 2$	6/3/*o*1	*Imma* 4(*e*)
1.6	*ABCEK*	$c = 1$	7/3/*o*4	*Pnna* 8(*e*)
1.7	*ABCEG*	$y = 0$; $c = 1$	6/4/*o*1	*Imma* 8(*h*)
1.8	*ABCEF*	$z = \frac{1}{4}$; $c = 1$	6/3/*o*2	*Cmcm* 8(*f*)
1.9	*ABCFKM*	$z = \frac{1}{4}$	8/3/*o*2	*Cmcm* 8(*f*)
1.10	*ABCFL*	$x = 0$, $z = \frac{1}{4}$; $a = c$	5/4/*t*6	*I*4/*mmm* 4(*e*)
1.11	*ABCFG*	$y = 0$, $z = \frac{1}{4}$; $b = 2$	5/4/*h*5	*P*6/*mmm* 2(*c*)
1.12	*ABCGL*	$x = y = 0$; $a = 2$	5/4/*h*5	*P*6/*mmm* 2(*c*)
1.13	*ABCGH*	$y = 0$; $b = 1$	6/3/*o*3	*Imma* 8(*h*)
1.14	*ABCHL*	$x = 0$; $b = 1$	6/4/*o*2	*Cccm* 8(*l*)
1.15	*ABCHIJ*	$y = \frac{1}{4}$; $b = 1$	7/3/*o*2	*Cmcm* 8(*g*)
1.16	*ABCIJLO*	$x = 0$, $y = \frac{1}{4}$; $c = a+2$	7/4/*o*1	*Fmmm* 8(*g*)
1.17	*ABCIJK*	$y = \frac{1}{4}$	7/3/*o*3	*Cmcm* 8(*g*)
1.18	*ABCKL*	$x = 0$; $a = 2^{-1/2}$	6/3/*t*5	$P\bar{4}m2$ 4(*j*)
0.1	*ABCDEK*	$\frac{1}{8}$, $\frac{1}{8}$, 0; 2, $2\times3^{1/2}$, 1	8/3/*t*1	$I4_1/amd$ 4(*a*)
0.2	*ABCDEGN*	$\frac{1}{8}$, 0, 0; 4, $3^{1/2}$, 1	8/3/*h*4	*P*6/*mmm* 1(*a*)
0.3	*ABCDGHN*	$\frac{1}{8}$, 0, 0; 4, 1, $3^{1/2}$	8/3/*h*4	*P*6/*mmm* 1(*a*)
0.4	*ABCDHIJ*	$\frac{1}{8}$, $\frac{1}{4}$, 0; $2\times3^{1/2}$, 1, 2	8/3/*h*4	*P*6/*mmm* 1(*a*)
0.5	*ABCDIJK*	$\frac{1}{8}$, $\frac{1}{4}$, 0; 2, $3^{1/2}$, 2	8/3/*h*4	*P*6/*mmm* 1(*a*)
0.6	*ABCEFG*	$\frac{1}{2}\times3^{1/2}-\frac{3}{4}$, 0, $\frac{1}{4}$; $2+3^{1/2}$, 2, 1	7/3/*o*1	*Cmmm* 4(*g*)
0.7	*ABCEFKM*	$\frac{1}{12}$, $\frac{1}{4}\times6^{1/2}-\frac{1}{2}$, $\frac{1}{4}$; $3^{1/2}$, $2+\frac{2}{3}\times6^{1/2}$, 1	10/3/*h*2	$P6_3/mmc$ 4(*f*)
0.8	*ABCFKLM*	0, $\frac{1}{4}\times2^{1/2}-\frac{1}{4}$, $\frac{1}{4}$; $2^{1/2}$, $2+2^{1/2}$, $2^{1/2}$	9/3/*t*2	*I*4/*mmm* 4(*e*)
0.9	*ABCFGL*	0, 0, $\frac{1}{4}$; 2, 2, 2	6/4/*c*1	*P*4/*mmm* 1(*a*)
0.10	*ABCGHL*	0, 0, $1-\frac{1}{2}\times3^{1/2}$; 2, 1, $2+3^{1/2}$	7/3/*o*1	*Cmmm* 4(*g*)
0.11	*ABCHIJLO*	0, $\frac{1}{4}$, $\frac{1}{2}\times3^{1/2}-\frac{3}{4}$; $3^{1/2}$, 1, $2+3^{1/2}$	9/3/*o*1	*Fmmm* 8(*g*)
0.12	*ABCIJKLO*	0, $\frac{1}{4}$, $\frac{1}{4}\times2^{1/2}-\frac{1}{4}$; $2^{1/2}$, $2^{1/2}$, $2+2^{1/2}$	9/3/*t*2	*I*4/*mmm* 4(*e*)

4. The transition mechanism

The ideal diamond arrangement belongs to sphere-packing type 4/6/*c*1 (2.1) with $x = \frac{1}{8}$, $y = \frac{1}{8}$, $z = 0$, $a/c = 2$ and $b/c = 2^{1/2}$, whereas the ideal lonsdaleite arrangement belongs to 4/6/*h*2 (2.3) with $x = \frac{1}{12}$, $y = \frac{1}{16}$, $z = \frac{1}{4}$, $a/c = 3^{1/2}$ and $b/c = \frac{2}{3}\times6^{1/2}$ (*cf.* above and Fig. 1). In principle, the transition between both types may happen along any one-dimensional path through the three-dimensional parameter field of sphere-packing type 3/10/*o*1. To pick out a particular transition path, two further parameter conditions have to be chosen in addition to (1). As each sphere in a diamond or in a lonsdaleite arrangement has 12 spheres with equal distances in its second coordination shell, the obvious procedure would be to postulate the equality of as many of these distances as possible. Only six of these distances may really become equal. They belong to three pairs of neighbouring spheres that, owing to symmetry, are always located at exactly equal distances from the reference sphere: $d_1^2 = 4x^2a^2 + \frac{1}{4}b^2 + \frac{1}{4}c^2$, $d_2^2 = \frac{1}{4}a^2 + 4z^2c^2$ and $d_3^2 = c^2$. On condition that all three pairs are equidistant, the following equations are valid:

$$d_1 = d_2 \quad \text{and} \quad d_1 = d_3. \tag{2}$$

Apart from the absolute sizes of the spheres and of the unit cell, the four equations of (1) and (2) describe a certain

transition path, *i.e.* they pick out exactly one particular sphere packing of type 3/10/*o*1 if, for example, a value of z is given.

Figs. 4, 5 and 6 show the variations depending on z of the coordinate parameters x and y, the axial ratios a/c and b/c, and the sphere-packing density ρ, respectively, along the proposed transition path.

The absolute sizes of the spheres and of the unit cell may be fixed in different ways, *e.g.* one may keep the radii of the spheres constant along the whole transition path,

$$r_{\text{sphere}} = \tfrac{1}{2}. \tag{3}$$

As a consequence, the three shortest distances between spheres also remain constant during the transition,

$$d_A = d_B = d_C = 1. \tag{4}$$

In this way, a possible transition path from a diamond sphere packing *via* sphere packings of type 3/10/*o*1 into an ideal lonsdaleite sphere packing is completely fixed. Figs. 7(*a*)–7(*e*) illustrate this sphere-packing deformation for some selected z values. The three shortest distances per sphere within a 3/10/*o*1 packing are drawn in black, the additional fourth shortest distance in the diamond or in the lonsdaleite arrangement is marked in blue or in green, respectively.

The sphere-packing deformation and the changes in the second coordination shell are reflected in the deformation of the corresponding Dirichlet domains (Figs. 7*f*–7*j*). For a diamond configuration, the Dirichlet domain (Fig. 7*f*) is a truncated tetrahedron with four large hexagons corresponding to the sphere-packing neighbours and 12 small triangular faces belonging to the 12 neighbours from the second coordination shell. As the lines joining the central atom with its neighbours from the second coordination shell do not pass through the corresponding faces, all these neighbours are so-called indirect neighbours. The Dirichlet domain for an ideal lonsdaleite arrangement (Fig. 7*j*) is also a truncated tetrahedron, but with three large hexagons, one large nonagon and seven small triangles, *i.e.* only part of the 12 neighbours from the second coordination shell give rise to faces of the Dirichlet domain. Six of the triangular faces refer to indirect neighbours, whereas the seventh triangle located opposite to the nonagon belongs to a fifth direct neighbour. In Figs. 7(*f*)–7(*j*), the three large faces corresponding to the black lines in Figs. 7(*a*)–7(*e*) are coloured in grey, those faces belonging to the blue and green lines are drawn in blue and green, respectively. The green face develops from a vertex of the diamond polyhedron, the blue face from an edge of the lonsdaleite polyhedron.

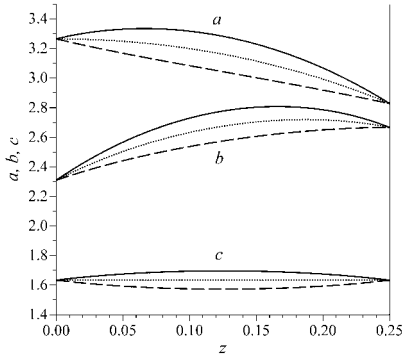

Figure 8
Variations of the lattice parameters a, b and c depending on z along the proposed transition path. Full lines refer to the additional condition $r_{\text{sphere}} = \frac{1}{2}$, dotted lines to $c = \frac{2}{3} \times 6^{1/2}$, and dashed lines to $V = \frac{64}{9} \times 3^{1/2}$.

As Fig. 7 illustrates, during the phase transition the relative position of each sphere changes only little with respect to all its neighbouring spheres but, simultaneously, the size and the shape of the unit cell of *Pnna* varies.

Fig. 8 shows the dependence of the lattice parameters a, b and c on z along the proposed transition path, and Fig. 9 shows the corresponding changes of the volume $V = abc$ of the unit cell of *Pnna* (full lines). During the phase transition, V increases by about 25.5%.

The changes of the distances between the original sphere and some neighbouring spheres during the phase transition are displayed in Fig. 10. It is noteworthy that one neighbour from the first coordination shell in a diamond configuration switches to the third coordination shell in an ideal lonsdaleite configuration, and *vice versa*. Furthermore, 10 of the 12 neighbours from the second coordination shell in a diamond arrangement enter the second coordination shell in a lonsdaleite arrangement. This means that 10 of the 12 nearest neighbours of like atoms in an AB compound are preserved during a transition from the zinc-blende to the wurtzite type according to the proposed model.

Instead of (3), one may use one of the following conditions to fix the sizes of the spheres and the unit cell for each given value of z,

$$c = c(z = 0) = c(z = \tfrac{1}{4}) = \tfrac{2}{3} \times 6^{1/2} \tag{5}$$

or

$$V = V(z = 0) = V(z = \tfrac{1}{4}) = \tfrac{64}{9} \times 3^{1/2}. \tag{6}$$

In comparison with (3), equation (5) leads to slightly smaller lattice parameters (*cf.* dotted lines in Fig. 8) and to an increase of the unit-cell volume by only 12.2% (*cf.* dotted line in Fig. 9) during the phase transition. As a consequence, the distances between the centres of spheres (Fig. 11) become shorter.

Equation (6) yields even smaller lattice parameters (*cf.* dashed lines in Fig. 8) and distances between spheres (Fig. 12) than equation (5).

The real path for a particular phase transition, *i.e.* the conditions that are fulfilled in addition to (1), cannot be determined by a purely geometrical model, but possibly with the aid of energy calculations.

5. Discussion

The proposed model for a phase transition from the diamond to the lonsdaleite type has the following properties. During the whole transformation process, all atoms remain symmetrically equivalent with respect to the common subgroup *Pnna* of $Fd\bar{3}m$ and $P6_3/mmc$. Only one bond per atom in the diamond-

type structure has to be removed. All broken bonds run in only two directions and are arranged in pairs of planes perpendicular to the [100] direction of *Pnna*, *i.e.* perpendicular to one of the ⟨110⟩ directions of $Fd\bar{3}m$. For each such pair of neighbouring planes, all broken bonds are parallel (*cf.* Fig. 7*a*). During the transition, the atomic arrangement corresponds to a sphere packing of type 3/10/*o*1 and, therefore, the three-dimensional connection of the crystal structure *via* bonds is preserved. At a halfway stage of the transition, *i.e.* for $z = \frac{1}{8}$, each atom lies in the same plane with its three nearest neighbours which form an isosceles triangle. The next two neighbours are equidistant from the central atom (*cf.* Figs. 10–12) and are located on different sides of this plane (*cf.* Fig. 7*c*). Their distances are approximately 56% longer than the shortest three. One of these neighbours originates from the first coordination shell in the diamond-type structure, the other gives rise to the newly formed bonds in the lonsdaleite-type structure after the phase transition ($z = \frac{1}{4}$) is finished. These new bonds run in four different directions (*cf.* Fig. 7*e*).

The proposed transition model is diffusionless, *i.e.* only relatively small movements of all atoms in a cooperative manner are necessary. It results in the following orientation relations for the diamond- and the lonsdaleite-type unit cells: (i) $[001]_{cub} = [001]_{hex}$ and (ii) $[1\bar{1}0]_{cub} = [100]_{hex}$.

Such a transition path seems to be rather unlikely for substances showing distinct stacking faults. Only if the original crystals are relatively undisturbed may it possibly occur. For compounds with stacking faults, *e.g.* for ZnS, other transition mechanisms are more probable, *e.g.* a displacement of planes

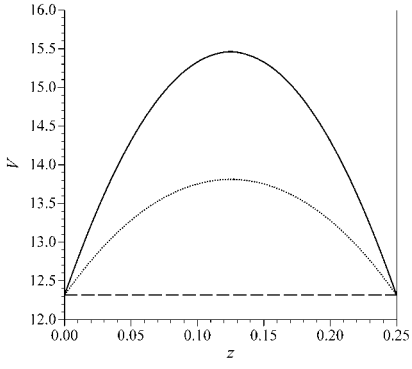

Figure 9
Variations of the volume V of a unit cell of *Pnna* depending on z along the proposed transition path. The full line refers to the additional condition $r_{sphere} = \frac{1}{2}$, the dotted line to $c = \frac{2}{3} \times 6^{1/2}$, and the dashed line to $V = \frac{64}{9} \times 3^{1/2}$.

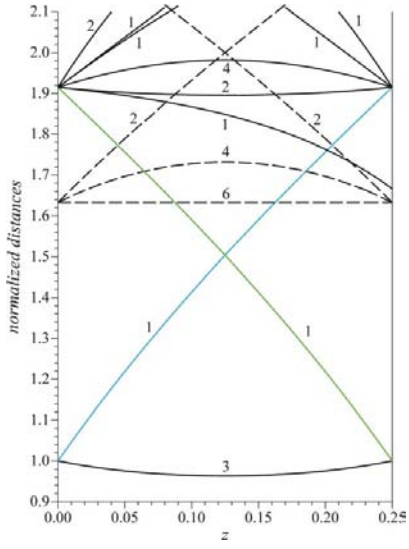

Figure 11
Variations of the interatomic distances depending on z along the proposed transition path. Additional condition: $c = \frac{2}{3} \times 6^{1/2}$. The blue and the green lines mark the distance to the lost neighbour in a diamond configuration and in an ideal lonsdaleite configuration, respectively.

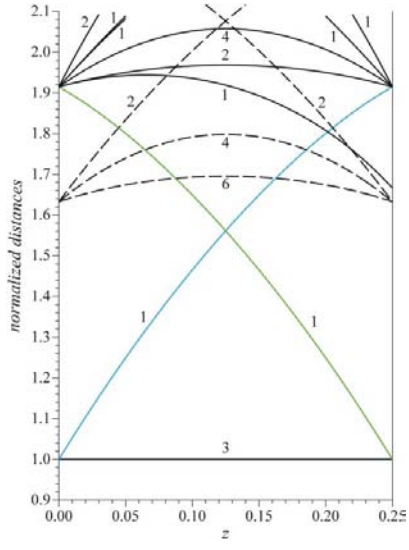

Figure 10
Variations of the interatomic distances depending on z along the proposed transition path. Additional condition: $r_{sphere} = \frac{1}{2}$. The blue and the green lines mark the distance to the lost neighbour in a diamond configuration and in an ideal lonsdaleite configuration, respectively.

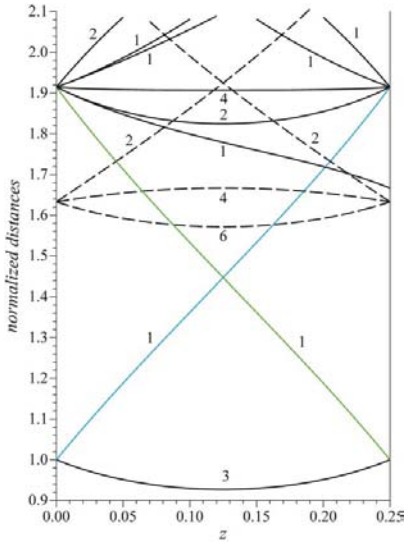

Figure 12
Variations of the interatomic distances depending on z along the proposed transition path. Additional condition: $V = \frac{64}{9} \times 3^{1/2}$. The blue and the green lines mark the distance to the lost neighbour in a diamond configuration and in an ideal lonsdaleite configuration, respectively.

of atoms parallel to $(111)_{cub}$ or $(001)_{hex}$, as proposed by Shôji (1931), or a martensitic transformation, as described by Pandey & Lele (1986). In both cases, the hexagonal **c** direction runs parallel to a cubic ⟨111⟩ direction. Of course, it is conceivable that the proposed transition model occurs for other *AB* compounds that do not tend to form stacking faults. In such a case, however, the phase transition should not be induced by mechanical stress or deformation.

Eremenko & Nikitenko (1972) made rows of indentations on platelets of silicon single crystals. They observed two-dimensional defects which were interpreted as platelets of a new silicon phase belonging to the lonsdaleite type. They found the following orientation relations: (*a*) $[\bar{1}10]_{cub} = [100]_{hex}$ and (*b*) $[110]_{cub} = [001]_{hex}$. Relation (*a*) corresponds to relation (ii) for the transition model proposed in the present paper, but (*b*) and (i) differ. The observed orientation of the lonsdaleite-type silicon phase is rotated by an angle of 90° around a cubic ⟨110⟩ direction with respect to the orientation of the present model.

Tan *et al.* (1981) confirmed the observations of Eremenko & Nikitenko (1972) and proposed a corresponding transformation mechanism: similar to the present model, this mechanism treats all atoms in an analogous way during the transition, *i.e.*, in principle, it should be possible to describe it in some common subgroup (other than *Pnna*) of $Fd\bar{3}m$ and $P6_3/mmc$. As in the present model, one bond per atom must be removed and one new bond is formed, and all the broken bonds run in only two directions. They are arranged in planes perpendicular to one of the ⟨110⟩ directions of $Fd\bar{3}m$. All broken bonds out of the same plane are parallel, those belonging to neighbouring planes have different directions. In contrast to the present model, the crystal structure splits up into layers perpendicular, for example, to $[110]_{cub}$ or $[001]_{hex}$ during the phase transition. All newly formed bonds are parallel to $[001]_{hex}$.

The transformation model proposed by Tan *et al.* (1981) seems to require much stronger deformations of the crystal structure than the present model. Therefore, the latter mechanism may possibly be preferred if the phase transition is induced more gently.

Referring to the phase transition between cristobalite and tridymite, the present model implies that relatively few Si—O bonds must be broken, and that the O atoms have to move only a short distance. Since with $z = \frac{1}{8}$ the fourth and the fifth Si neighbours of each Si atom are equidistant, all O atoms corresponding to the 'blue bonds' in Fig. 7 should move simultaneously to the centres of the 'green bonds'. In this respect, the present model resembles the 'two-O-atom four-centre transition path' recently proposed by Leoni & Nesper (2000) for the quartz–tridymite transition.

We would like to thank Professor W. Fischer, Marburg, Germany, for many helpful discussions.

References

Allen, E. T. & Crenshaw, J. L. (1913). *Z. Anorg. Chem.* **79**, 125–189.
Eremenko, V. G. & Nikitenko, V. I. (1972). *Phys. Status Solidi A*, **14**, 317–330.
Fischer, W. (1971). *Z. Kristallogr.* **133**, 18–42.
Fischer, W. (1973). *Z. Kristallogr.* **138**, 129–146.
Fischer, W. (1991(*a*)). *Z. Kristallogr.* **194**, 67–85.
Fischer, W. (1991*b*). *Z. Kristallogr.* **194**, 87–110.
Fischer, W. & Koch, E. (1994). *Z. Kristallogr.* Suppl. Issue 9, 208.
International Tables for Crystallography (1995). Vol. A, edited by Th. Hahn. Dordrecht: Kluwer Academic Publishers.
Koch, E. & Fischer, W. (1995). *Z. Kristallogr.* **210**, 407–414.
Leoni, S. & Nesper, R. (2000). *Acta Cryst.* A**56**, 383–393.
Pandey, D. & Lele, S. (1986). *Acta Metall.* **34**, 415–424.
Sebastian, M. T., Pandey, D. & Krishna, P. (1982). *Phys. Status Solidi A*, **71**, 633–640.
Shallcross, F. V. & Carpenter, G. B. (1957). *J. Chem. Phys.* **26**, 782–784.
Shôji, H. (1931). *Z. Kristallogr.* **77**, 381–410.
Shôji, H. (1933). *Z. Kristallogr.* **84**, 74–84.
Sowa, H. (2000*a*). *Acta Cryst.* A**56**, 288–299.
Sowa, H. (2000*b*). *Z. Kristallogr.* **215**, 335–342.
Sowa, H. (2001). *Acta Cryst.* A**57**, 176–182.
Tan, T. Y., Föll, H. & Hu, S. M. (1981). *Philos. Mag. A*, **44**, 127–140.
Yeh, C. Y., Lu, Z. W., Froyen, S. & Zunger, A. (1992). *Phys. Rev. B*, **46**, 10086–10097.